



Removal of tetracyclines from aqueous solution by nanoscale Cu/Fe bimetallic particle

Sibel Aslan*, Kenan Yalçın, Özge Hanay, Burçin Yıldız

Faculty of Engineering, Department of Environmental Engineering, Firat University, Elazığ 23119, Turkey, Tel. +90 424 2370000, ext. 5622; Fax: +90 424 2415526; emails: sibela@firat.edu.tr (S. Aslan), kenan_1929@hotmail.com (K. Yalçın), Tel. +90 424 2370000, ext. 5623; Fax: +90 424 2415526; emails: ohanay@firat.edu.tr (Ö. Hanay), burcinyildiz23@gmail.com (B. Yıldız)

Received 10 September 2014; Accepted 21 June 2015

ABSTRACT

Bimetallic nanoparticle (BNP) that comprises nanoscale zero-valent iron with a noble metal such as Pd, Pt, Ni, Ag, or Cu has been effective in removing various organic and inorganic compounds. In this study, the removal performance of tetracycline antibiotics, tetracycline (TC), oxytetracycline (OTC), and chlortetracycline (CTC), from aqueous solution by nanoscale copper/iron (Cu/Fe) bimetallic particle was investigated. Batch experiments were performed to evaluate the effect of experimental variables such as solution pH, bimetallic particle dosage, and temperature on the removal efficiency of tetracyclines. The results obtained from the study indicated that the removal rate of tetracyclines was greatly dependent on pH. The removal of TCs above 90% was achieved at optimum conditions. The Langmuir and Freundlich adsorption models were applied to experimental data and the results fitted to Langmuir model. The pseudo-first-order and the pseudo-second-order models were used to express of adsorption kinetics and it was found that the adsorption kinetics were followed the pseudo-second-order kinetic model.

Keywords: Tetracycline; Oxytetracycline; Chlortetracycline; Nanoscale zero-valent iron; Copper/iron bimetallic particle

1. Introduction

Pharmaceuticals in general are biologically active compounds that are intended not to be easily biodegradable and are often water soluble and therefore they can be found in wastewaters and can easily end up in natural waters [1]. In some cases even drinking water is contaminated with pharmaceuticals [2]. Depending on their physicochemical properties such as aqueous solubility, volatility, and lipophilicity,

pharmaceuticals could be subjected to several treatment processes during wastewater treatment [3]. However, since most pharmaceuticals feature a high persistency and polarity, many of them are not or only incompletely removed by conventional biological wastewater treatments [4]. Therefore, it is of great importance to develop alternative treatment technologies for effective removal of these compounds [5].

Antibiotics that are one group of pharmaceuticals inhibit or abolish the growth of micro-organisms, such as bacteria, fungi, or protozoa. They are used extensively in human and veterinary medicine, as well as

*Corresponding author.

in aquaculture, for the purpose of preventing or treating microbial infections. There are various subgroups of antibiotics such as β -lactams, quinolones, tetracyclines, macrolides, sulphonamides, and others [6]. Tetracyclines (TCs) including tetracycline (TC), oxytetracycline (OTC), and chlortetracycline (CTC) are the second most widely used antibacterial compounds in the world due to their broad spectrum, high quality and low price [7,8]. They are used to treat diseases in humans and also applied to livestock to prevent disease and promote growth [5,9]. TCs have a high aqueous solubility and a long environmental half-life [10]. The presence of TCs in natural environments can cause bacteria to acquire and transmit antibiotic-resistant genes, which potentially threaten ecosystem functions and human health [11]. In recent years, the various removal techniques such as advanced oxidation/reduction [5], ozonation [12,13], coagulation, and granular activated carbon filtration [14,15], adsorption by various adsorbents including activated carbon [16], multi-walled carbon nanotubes [17], have been used to remove TCs from water.

Zero-valent iron (ZVI) particles were introduced by Gillham and O'Hannesin [18] and then they are increasingly being used for environmental remediation [19]. Nanoscale zero-valent iron (nZVI) was first tested for contaminated water treatment by Wang and Zhang [20]. Since then nZVI technology has received much attention for soil and groundwater remediation and wastewater treatment because of their advantages such as enhanced reactivity by increasing the surface to volume ratios, and providing more reactive surface sites as compared with the bulk or microscale iron particles [21], rapid reaction rate, low apparatus cost, and no need of additional chemical additives [22]. nZVI is highly effective for the removal of a variety of pollutants such as chlorinated solvents, chlorinated pesticides, azo dyes, organophosphates, nitroamines, nitroaromatics, polybrominated diphenyl ethers, polychlorinated biphenyls, nitrate, and perchlorate, as well as heavy metals [22,23]. nZVI can either remove contaminants through reduction or adsorption [24]. Ghauch et al. [25] showed that β -lactams were successfully removed by microscale and nanoscale iron particles.

Bimetallic nanoparticle (BNP) is a combination of nZVI with a noble metal such as Pd, Pt, Ni, Ag, or Cu [26]. The noble metal promotes iron oxidation and may act as a catalyst for electron transfer and hydrogenation [26–29]. BNP has some advantages such as cost effectiveness, good corrosion stability, high reactivity, and faster contaminant degradation [29,30]. Moreover, nano Fe is nontoxic because it can be oxidized to naturally occurring soil mineral components.

Bimetallic Fe nanoparticles are widely used in the catalytic elimination of various pollutants [30].

There are a few studies investigating the removal of antibiotics such as metronidazole [31,32], amoxicillin, and ampicillin [25] by nZVI. Up to now, reports on the use of bimetallic particles for antibiotic elimination from water are scarce. Raja et al. [33] investigated the removal of antibiotic metronidazole from water using bimetallic Fe/Pd nanoparticles. This paper aims to investigate the removal of TCs from aqueous solution by nanoscale Cu/Fe bimetallic particle. For this aim, batch experiments were carried out to investigate the effect variables such as solution pH, nanoscale Cu/Fe bimetallic particle dosage, and temperature on removal of three tetracyclines (TC, OTC, and CTC) by nanoscale Cu/Fe bimetallic particle. Moreover, it was tried to determine the removal mechanism of TCs by analyzing transformation products at optimum conditions.

2. Materials and methods

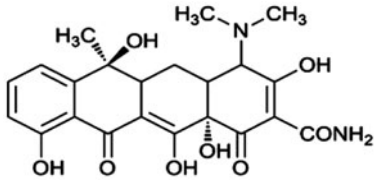
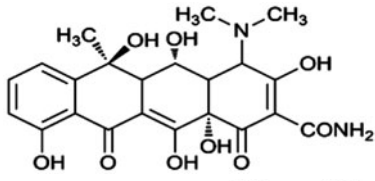
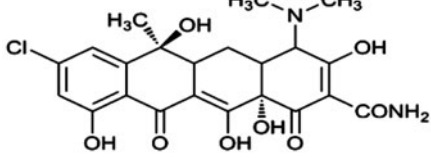
2.1. Reagents

The solutions of tetracycline, chlortetracycline, and oxytetracycline were prepared from hydrochloride salts purchased from Applichem and Sigma. The properties of TC, OTC, and CTC are summarized in Table 1. The pH-dependent speciation of tetracyclines is given in Fig. 1 [34]. Methanol, acetonitrile, and formic acid from Merck were high performance liquid chromatography (HPLC) and liquid chromatography-mass spectrometry (LC-MS) grade and other reagents were also in analytical grade. Reagent water was produced from a Millipore Milli-Q Ultrapure Gradient 3 V purification system. Deionized deoxygenated water was used to prepare the solutions, and solutions were stored at 4°C until use.

2.2. Preparation of nZVI and nanoscale Cu/Fe bimetallic particle

nZVI particles used in the experiments were prepared using method given by Hwang et al. [35]. nZVI was synthesized in a 500 mL flask reactor with four open necks. One of the necks housed a tunable mechanical stirrer and the solution was stirred vigorously at 250 rpm. For the reduction of ferric ions to nZVI, a peristaltic pump was used to introduce 250 mL of borohydride solution into 250 mL of ferric ions solution. Two remain necks provided the inlet and outlet of nitrogen gas to prevent any possible oxidation of iron. nZVI synthesis conditions were as follows: reductant delivery rate: 20 mL min⁻¹, [Fe³⁺]:

Table 1
Characteristics of tetracyclines

Tetracyclines	Molecular formula	Molecular weight (g mol ⁻¹)	Chemical structure
Tetracycline	C ₂₂ H ₂₄ N ₂ O ₈	444.435	
Oxytetracycline	C ₂₂ H ₂₄ N ₂ O ₉	460.434	
Chlortetracycline	C ₂₂ H ₂₃ ClN ₂ O ₈	478.880	

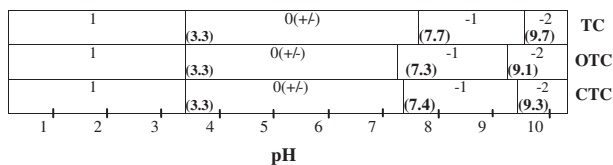
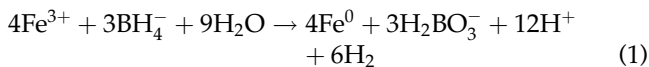


Fig. 1. The pH-dependent speciation of tetracycline antibiotics (the values in parenthesis represent the pK_a values of TCs).

71.7 mM and [BH₄⁻]: 358.5 mM. The reduction reaction can be described as follows:



The resulting gray-black nZVI was collected by vacuum filtration of the solution. The collected particles were then washed three times with ethanol, dried, and stored in an anaerobic chamber.

Bimetallic particle was prepared according to the method given by Fennelly and Roberts [36]. A dilute solution (50 μM) of CuSO₄ was added slowly to 2-g nZVI and the solution was agitated. To precipitate of second metal onto the nZVI was waited for a few minute. After metal was rinsed with deoxygenated water and acetone and, it was completely dried on 60–65°C and preserved under nitrogen gas. The copper amount

of filtrate was analyzed to verify whether all of the copper was completely precipitated onto the iron. The residual copper concentration of filtrate in the solution was negligible. The concentration of copper in the bimetallic particle was 0.035% mol.

2.3. Batch experiments

The batch experiments were carried out in 120-mL glass beakers containing appropriate amounts of bimetallic particle and 100 mL solutions of TCs having different concentrations and pH. The glass beakers were wrapped with aluminum foil to prevent them from light, and they were put in ultrasonic cleaning bath (Jeiotech) to ultrasonically disperse the bimetallic particle. The reaction mixtures were shaken at 150 rpm using a constant temperature orbital shaker (Gallenkamp) for different reaction times. At the end of the predetermined time intervals, the samples were withdrawn by syringe, filtered through 0.22 μm membrane filter and analyzed for TCs. The control test was carried out according to the same procedure and monitored the stability of TCs in the absence of bimetallic particle. All experiments were repeated twice for reproducibility results and average results were represented.

The influence of operation parameters such as pH, bimetallic particle dosage, and temperature was investigated by batch experiments. In order to evaluate the influence of initial pH on the removal of TCs,

bimetallic particle dosage of 0.4 g L^{-1} added in solutions containing 60 mg L^{-1} TCs with the initial pH values varying from 2 to 9. The solution pH was adjusted to the desired values using diluted HCl or NaOH solutions. The effect of bimetallic particle dosage was investigated at different dosages between 0.1 and 1 g L^{-1} , and 60 mg L^{-1} TCs concentration for different contact times. The initial pH of TC solutions was adjusted to optimum values that found for each TC at previous stage. The effect of temperature was examined at temperatures of 30, 45, and 60°C .

The TCs removal yield was calculated as follows:

$$\text{Removal \%} = \frac{C_0 - C_t}{C_0} \times 100 \quad (2)$$

The amount of TCs adsorbed per gram of bimetallic particle at any time, q_e was calculated as follows:

$$q_e = \frac{V \cdot (C_0 - C_e)}{m} \quad (3)$$

where C_0 and C_e are the initial and equilibrium concentrations of TCs (mg L^{-1}), V is the volume of solution (L), and m is the mass of bimetallic particle (g).

The adsorption isotherms experiments were carried out at different initial TCs concentrations varying from 20 to 100 mg L^{-1} . The glass beakers were placed in orbital shaker at temperature of 30, 45, and 60°C . After determined equilibrium time was reached, samples were taken and concentrations of TCs were determined.

Desorption studies were carried out to desorb TCs from Cu/Fe bimetallic particle surface. Ten microliters of concentrated HCl was added to 1 mL of sample aliquot and it was shaken for 3 min. Then, the sample centrifuged for 20 min and TC concentration of supernatant was analyzed by HPLC.

2.4. Analytical methods

The size and elemental content of nanoscale Cu/Fe bimetallic particle were determined using scanning electron microscopy (Jeol-JSM-7001F). The specific surface was analyzed with a Brunauer–Emmett–Teller (BET) surface area analyzer. The heavy metal analysis of filtrate in aqueous solution was carried out by atomic absorption spectroscopy (Perkin Elmer 400). Analysis of TCs was performed by HPLC (Shimadzu) with column AllureBiPh ($5 \mu\text{m}$, $150 \times 4.6 \text{ mm}$). The mobile phase was composed of a mixture of ammonium dihydrogenphosphate/acetonitrile (20/80, v/v). The flow rate and sample size were 1.2 mL min^{-1} and: $100 \mu\text{L}$, respectively. TCs were detected at 269 nm by a

diode-array detector. The retention time of TC, OTC, and CTC were 3.90, 3.05, and 7.07 min, respectively. Calibration was made five standards between 20 and 100 mg L^{-1} with an r^2 no less than 0.998. pH values of solutions were measured with a pH-meter (Orion 3 STAR). pH_{ZPC} analysis was carried out according to the method used by Kumar and Porkodi [37].

The transformation products of TCs was analyzed by LC-MS-MS (Shimadzu LC-20 AD) with Venusil XBP C18 column ($3 \mu\text{m}$, 100 \AA , $2.1 \times 50 \text{ mm}$). The injection volume was $100 \mu\text{L}$. Two mobile phases were used to separate target compounds. Mobile phase A consisted of a mixture of 0.1% formic acid (v/v) and ultrapure water, while mobile phase B consisted of a mixture of 0.1% formic acid (v/v) and methanol. The linear gradient elution was as follows: the initial 5% B was increased to 15% within 6 min, a further 25% B was increased 40% in 6 min. Finally, the gradient was returned to the initial conditions of 5% B for 13 min. The flow rate was 0.3 mL min^{-1} at the column temperature of 40°C .

3. Results and discussions

3.1. Characterization of Cu/Fe bimetallic particles

The SEM image shown in Fig. 2 indicates that synthesized nanoscale Cu/Fe bimetallic particles clustered and agglomerated due to the magnetic interactions between the metallic particles. The particle size of synthesized Cu/Fe bimetallic was between 620 and $5,040 \text{ nm}$. The specific surface area of bimetallic particle was $25 \text{ m}^2 \text{ g}^{-1}$. The EDX graph and elemental content of Cu/Fe bimetallic particle are given in Fig. 3 and Table 2, respectively. The nanoscale bimetallic particle included 93.38% Fe and 3.67% oxygen due to

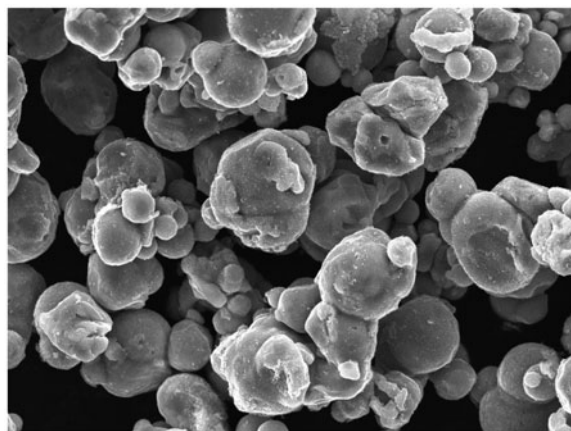


Fig. 2. SEM image of nanoscale Cu/Fe bimetallic particle.

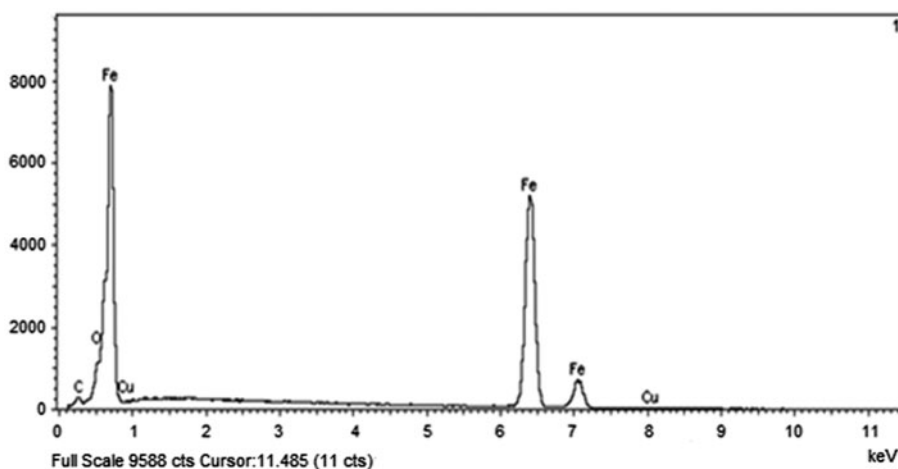


Fig. 3. EDX graph of nanoscale Cu/Fe bimetallic particle.

Table 2

The elemental content of nanoscale Cu/Fe bimetallic particle.

Element	% of weight	% of atomically
C	2.83	11.02
O	3.67	10.72
Fe	93.38	78.17
Cu	0.12	0.09
Total	100.00	100.00

the oxidation of Fe during sample preparation and processing of the material for SEM analysis. The Cu content of bimetallic particle was found as 0.12%. pH_{ZPC} value of Cu/Fe bimetallic particle was found to be 7.0.

3.2. The influence of operational parameters on TCs removal

3.2.1. Influence of solution pH

It is well known that pH value of aqueous solution is one of the most important parameters that affect the removal of contaminants using Fe^0 from water. The effect of pH on removal of TCs by nanoscale Cu/Fe bimetallic particle was investigated at the initial pH range varying from 2 to 9. The batch experiments were carried out with initial TCs concentrations of 60 mg L^{-1} at 30°C and the results are presented in Fig. 4. When the initial pH increased, the removal of TCs increased and the highest removal efficiencies were usually obtained at pH of 6. Tetracyclines have several polar and ionizable functional groups including amino, carboxyl, phenol, alcohol, and ketone and

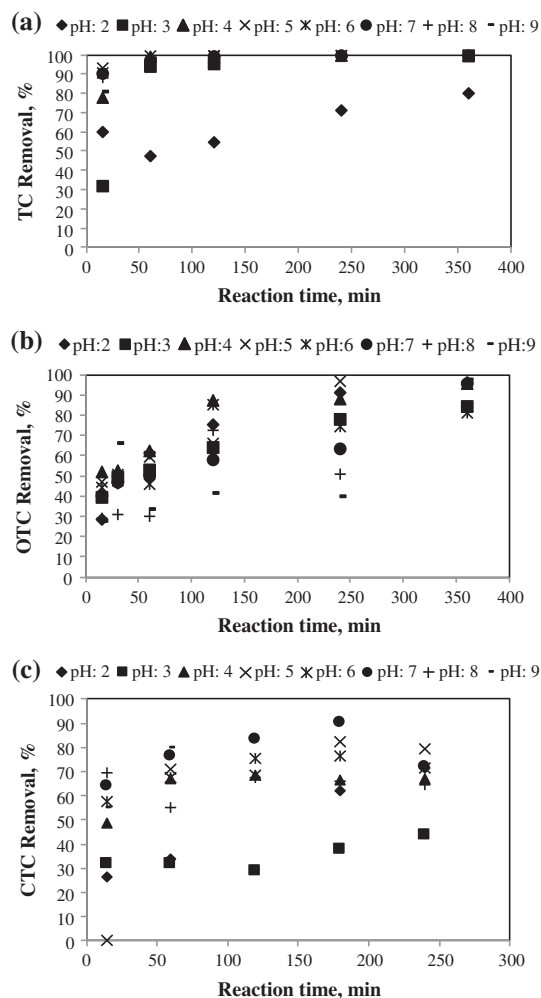


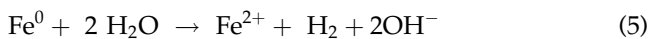
Fig. 4. Effect of initial solution pH on removal of TC (a), OTC (b), and CTC (c) (conditions: $\text{ZVI} = 0.4 \text{ g L}^{-1}$, $\text{C}_{0(\text{TCs})} = 60 \text{ mg L}^{-1}$, $T = 30^\circ\text{C}$).

Table 3
The final pH values of TC, OTC, and CTC solutions

Initial pH	Final pH		
	TC	OTC	CTC
2	2.31	2.07	2.14
3	3.02	3.44	3.29
4	5.37	5.08	4.50
5	6.27	6.25	6.04
6	6.77	6.50	6.40
7	7.02	6.65	6.93
8	7.57	7.37	7.42
9	8.16	7.94	8.05

the charge of the molecules depend on the solution pH [7]. They have three pKa values and the pKa values were 3.3, 7.7, 9.7 for TC, 3.3, 7.3, 9.1 for OTC and 3.3, 7.4, 9.3 for CTC [38]. Therefore, they can exist as cationic, zwitterionic, or anionic species under acidic, moderately acidic to neutral, and alkaline conditions, respectively. Since pH_{ZPC} value of Cu/Fe bimetallic particle was 7.0, it is positively charged at $pH < 7.0$ and negatively charged at $pH > 7.0$. Therefore, the higher removal of TCs at pH values higher than five can be attributed to electrostatic interaction. The similar result was obtained from the study of Gu and Karthikeyan [39] investigating tetracycline sorption on hydrous oxide of Al (HAO). Li et al. [10] obtained about 80% TC removal using kaolinite at pH 7.

The final pH values of all solutions at the end of the reactions are given in Table 3. It was observed that the final pH values increased until initial pH 7 and then decreased. The cause of pH increase is that in the absence of O_2 , according to Eq. (4), Fe^0 is oxidized to Fe^{2+} and H^+ is reduced to H_2 , then according to Eq. (5) the reduction of H_2O generates OH^- .



3.2.2. Influence of nanoscale bimetallic Cu/Fe dosage

The influence of bimetallic particle dosage on the removal of TCs was investigated at different dosages between 0.1 and 1 g L^{-1} within 2 h. At this stage, pH of TC solutions was adjusted to optimum pH value that obtained at previous stage. As seen from Fig. 5(a)–(c), the removal efficiencies of TCs increased when bimetallic particle dosages increased. This increase in TCs removal could be attributed to the

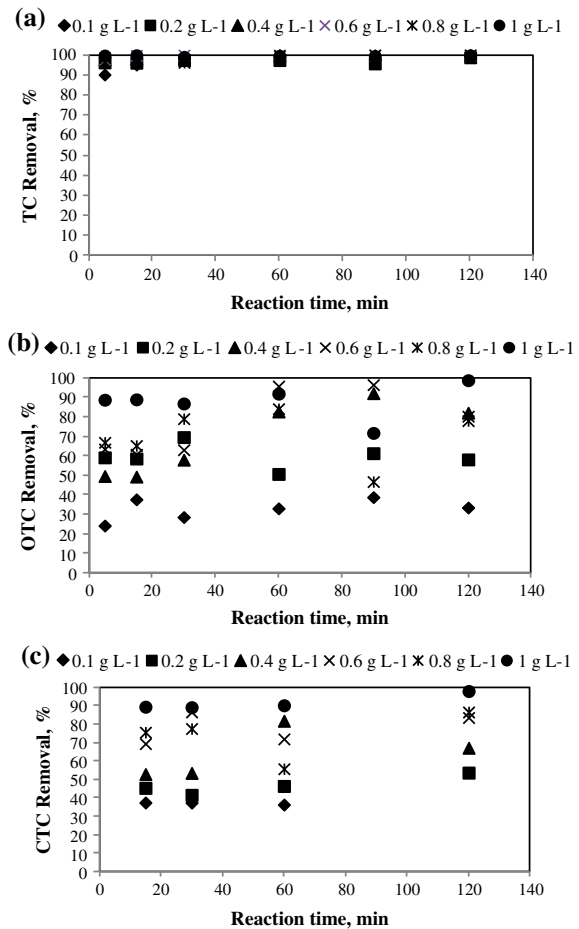


Fig. 5. Effect of nanoscale Cu/Fe bimetallic particle dosage on the removal of TC (a), OTC (b), and CTC (c) (conditions: pH 6, $C_{0(TCs)} = 60 \text{ mg L}^{-1}$, $T = 30^\circ\text{C}$).

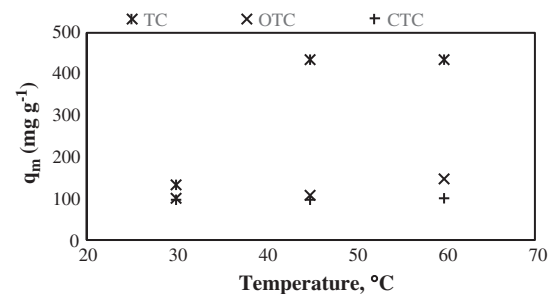


Fig. 6. Effect of temperature on the removal of TCs (conditions: pH 6, $C_{0(TCs)} = 60 \text{ mg L}^{-1}$, ZVI dosage = 0.2 g L^{-1} (for TC), and 0.6 g L^{-1} (for OTC and CTC)).

increase in active adsorption sites of bimetallic particle. TC removals were close to each other at all dosages and generally they were above 90% for all of

the time intervals. The optimum bimetallic particle dosage for TC, OTC, and CTC was found as 0.2, 0.6, and 0.6 g L⁻¹, respectively.

3.2.3. Influence of temperature

The effect of temperature on removal of TCs was investigated in the temperature 30, 45, and 60 °C at 60 mg L⁻¹ initial TCs concentrations. It can be seen from Fig. 6 that as the temperature increased from 30 to 45 °C, removal efficiency of TCs increased. This increase can be explained with increase in mobility of TCs from solution to bimetallic particles and acceleration of iron corrosion at higher temperatures. Moreover, the temperature rising may promote electrostatic attraction or chemical binding [40]. As similar our results were obtained in the study of Chen et al. [41] who investigated the removal of tetracycline by polyvinylpyrrolidone modified nZVI.

3.3. Adsorption kinetics

The adsorption kinetics that describes the solute uptake rate governing the residence time of the sorption reaction is an important characteristic that defines the efficiency of sorption [42]. Pseudo-first-order and pseudo-second-order rate models are used to determine kinetic parameters and describe the adsorption mechanism. The pseudo-first-order kinetic model is also known as the Lagergren model and is widely used adsorption rate equation for the adsorption of solute from aqueous solution. Lagergren kinetic equation is given by

$$\frac{dq}{dt} = k_1(q_{eq} - q) \quad (6)$$

where q_{eq} and q is adsorbed TCs quantity per gram of Cu/Fe bimetallic particle at equilibrium and any time (mg g⁻¹), respectively, k_1 is the rate constant of pseudo-first-order sorption (min⁻¹). Eq. (6) can be integrated for the boundary conditions $t = 0$ to $t = t$, $q = 0$ to $q = q_t$, it becomes,

$$\log(q_{eq} - q) = \log(q_{eq}) - \frac{k_1}{2.303}t \quad (7)$$

A plot of $\log(q_{eq} - q)$ against t should give a linear relationship with the slope of $k_1/2.303$ and intercept of $\log(q_{eq})$.

The pseudo-second-order kinetic model is also based on the adsorption capacity of the solid phase and the assumption that the adsorption process

involves chemisorption mechanism. It can be expressed by the following differential equation:

$$\frac{dq}{dt} = k_2(q_{eq} - q)^2 \quad (8)$$

where k_2 is the rate constant of pseudo-second-order adsorption. Integrated Eq. (8) for initial condition $q = 0$ when $t = 0$, following equation is obtained:

$$\frac{t}{q} = \frac{1}{k_2 \cdot q_{eq}^2} + \frac{1}{q_{eq}}t \quad (9)$$

In the case of second-order kinetic equation, the plot of t/q against t of Eq. (9) should give a linear relationship that the q_{eq} and k_2 could be determined.

The plots of linear form of the pseudo-first-order and pseudo-second-order equations are given in Figs. 7 and 8, respectively. First-order kinetic model and second-order kinetic model coefficients are summarized

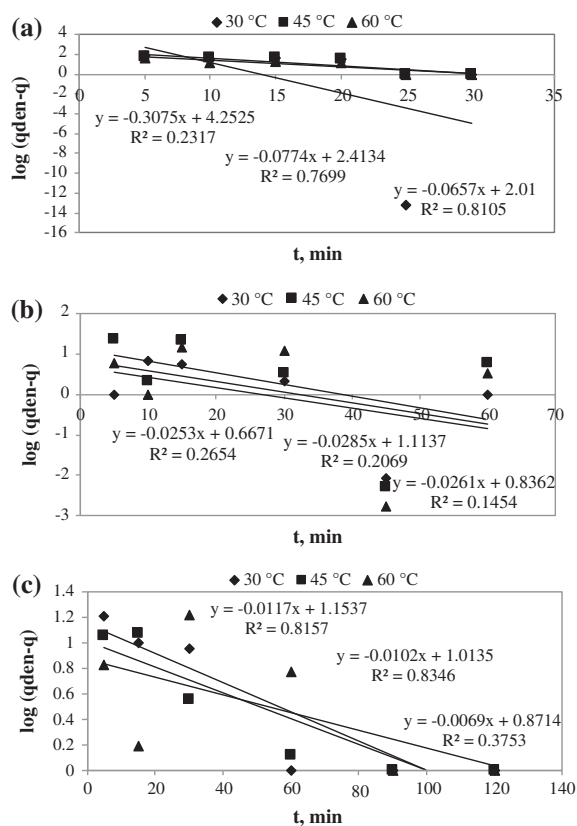


Fig. 7. Pseudo-first-order adsorption kinetics of TC (a), OTC (b), and CTC (c) at different temperatures (conditions: pH 6, $C_{0(TCs)}$ = 20–100 mg L⁻¹, ZVI dosage = 0.2 g L⁻¹ (for TC), 0.6 g L⁻¹ (for OTC and CTC)).

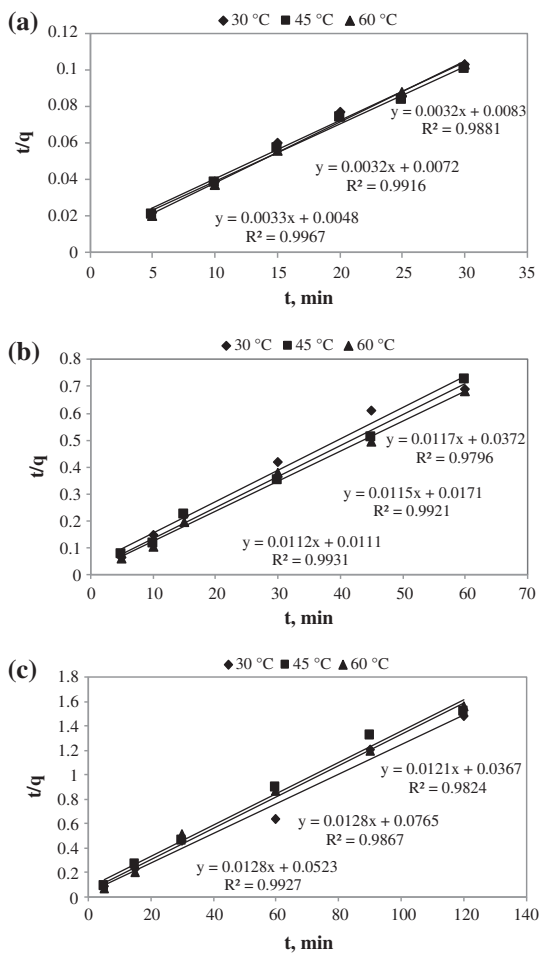


Fig. 8. Pseudo-second-order adsorption kinetics of TC (a), OTC (b), and CTC (c) at different temperatures (conditions: pH 6, $C_{0(\text{TCs})} = 20\text{--}100 \text{ mg L}^{-1}$, ZVI dosage = 0.2 g L^{-1} (for TC), 0.6 g L^{-1} (for OTC and CTC)).

in Table 4. According to the obtained results, our kinetic data complied very well with pseudo-second-order

kinetic model with correlation coefficient (R^2) higher than 0.98. The similar results as ours were also obtained by other researchers investigating TC removal by various adsorbents [40,42–44]. Sorption kinetics followed the pseudo-second-order model, suggesting that the adsorption rate-limiting step may be chemisorption and the adsorption of TCs occurs via surface complexation reactions at specific sorption sites [40]. As seen from Table 4, although the calculated q_{eq} values according to pseudo-second-order kinetic model were close to the experimental q_{eq} values, pseudo-first-order kinetic model did not agreed with experimental results.

3.4. Adsorption isotherms

Adsorption isotherms are used to investigate the relationship between the amount of contaminant adsorbed and the contaminant concentration remaining in the solution. The Langmuir and Freundlich isotherm equations are most frequently used to describe equilibrium adsorption isotherms. The linearized form of Langmuir isotherm equation is expressed as below:

$$\frac{C_e}{q_e} = \frac{1}{q_m \cdot K_b} + \frac{C_e}{q_m} \quad (10)$$

where q_m is the maximum monolayer adsorption (mg g^{-1}), C_e is the equilibrium concentration of TCs (mg L^{-1}), q_e is the amount of TCs adsorbed per unit weight of nZVI at equilibrium concentration (mg g^{-1}), and K_b is the Langmuir constant related to the affinity of binding sites (L mg^{-1}). Langmuir model suggests that the adsorption occurs through monolayer adsorption on homogeneous surface without transformation and interaction between sorbed molecules. When C_e/q_e is plotted against C_e , q_m , and K_b are determined the slope and intercept of the plot.

Table 4

The pseudo-first-order and the pseudo-second-order reaction rate constants at different temperatures

TCs	T (°C)	$q_{\text{eq,exp}}$ (mg g^{-1})	First-order kinetic model			Second-order kinetic model		
			k_1 (min^{-1})	$q_{\text{eq,cal}}$ (mg g^{-1})	R^2	k_2 ($\text{g mg}^{-1} \text{min}^{-1}$)	$q_{\text{eq,cal}}$ (mg g^{-1})	R^2
TC	30	293.10	0.71	70.28	0.2317	0.001	312.5	0.9881
	45	299.21	0.18	11.17	0.7699	0.001	312.5	0.9916
	60	284.40	0.15	7.46	0.8105	0.002	303	0.9967
OTC	30	73.81	1.95	0.058	0.2654	0.004	85.47	0.9796
	45	88.35	3.05	0.066	0.2069	0.008	86.96	0.9921
	60	91.24	2.31	0.06	0.1454	0.011	89.29	0.9931
CTC	30	74.52	0.027	3.17	0.8157	0.004	82.64	0.9824
	45	68.16	0.023	2.76	0.8346	0.002	78.13	0.9867
	60	75.14	0.016	2.39	0.3753	0.003	78.13	0.9927

Furthermore, the widely used empirical Freundlich model based on sorption on a heterogeneous surface, which suggests that binding sites are not equivalent and/or independent. The linearized form of Freundlich equation is expressed as:

$$\log q_e = \log K_F + (1/n) \cdot \log C_e \quad (11)$$

where K_F is an indicator of the adsorption capacity and n is an indicator of the adsorption intensity.

K_F and n constants are determined from the slope and intercept of the plot that is plotted $\log q_e$ vs. $\log C_e$.

The data obtained by applying Langmuir and Freundlich equations to the obtained results are presented in Table 5. Experimental data from adsorption of TCs on Cu/Fe bimetallic particle fitted to Langmuir isotherm model. Maximum adsorption capacity (q_m) at 30, 45, and 60 °C were 133.33, 434.78, and 435 mg g⁻¹ for TC, 101.01, 109.89, and 149.25 mg g⁻¹ for OTC, 100, 99, and 101.01 mg g⁻¹ for CTC, respectively. These values are higher than q_m obtained for TC by graphene oxide (313.48 mg g⁻¹) [45], illite (IMt-2) (32 mg g⁻¹) [43]. Also, in the study investigating the adsorption on nZVI of TC and OTC, q_m values at 30, 45, and 60 °C were found as 159, 208, and 233 mg g⁻¹ for TC and 110, 145, and 149 mg g⁻¹ for OTC [46]. However, the higher q_m value for OTC was obtained by graphene oxide (212.314 mg g⁻¹) [45]. In the study of Lin et al. [8], maximum adsorption capacities for TC, OTC, and CTC by graphene oxide functionalized magnetic particles were calculated as 39.1, 45.0, and 42.6 mg g⁻¹, respectively.

The Freundlich constant, n , were in the range of 1–10 and $n > 1$ represents favorable adsorption condition [47]. For all experiments in this study, n values were higher than unity. Therefore, it could be concluded that adsorption of TCs on Cu/Fe bimetallic particle is favorable.

3.5. Transformation products

It is crucial to analyze the transformation products to determine the removal mechanism and to assess the toxicology. In some cases, the transformation products may be more toxic than the parent compound. For this aim, the transformation products of TCs were analyzed at optimum removal conditions. The analyzed transformation products were 4-epi-tetracycline (ETC), 4-epi-anhydrotetracycline (EATC), anhydrotetracycline (ATC), 4-epi-oxytetracycline (EOTC), α -Apo-oxytetracycline (α -Apo-OTC) and β -Apo-oxytetracycline (β -Apo-OTC), 4-epi-chlortetracycline (ECTC), anhydrochlortetracycline (ACTC), and 4-epi-anhydrochlortetracycline (EACTC).

Transformation products of TCs can be formed via the epimerization, dehydration, and proton transfer pathways [48]. The concentrations of transformation products vs. reaction time were illustrated in Fig. 9. The initial concentration of TCs was 60 mg L⁻¹. The dominant transformation product of TC was ETC and its concentration was decreased within 30 min of reaction. TC, OTC, and CTC can be reversibly epimerized at position C-4 to form the corresponding four epimers (ETC, EOTC, and ECTC) in mildly acidic conditions (pH 2–6) [48]. The transformation products of OTC were EOTC, β -Apo-OTC, α -Apo-OTC, and their concentrations were increased with time except for EOTC and then were decreased. The dominant transformation product of CTC was ECTC, and its concentration of ECTC was decreased to 78.50 from 94 μ g L⁻¹ at the end of the reaction time. The concentrations of TC, OTC, and CTC transformation products during reaction time were significantly low. The desorbed percentage of TC, OTC, and CTC with acid desorption were 56.98, 52.87, and 66.39%. Therefore, it can be concluded that the removal of TCs was mainly resulted from adsorption on Cu/Fe bimetallic particle.

Table 5
Langmuir and Freundlich isotherm constants

TCs	T (°C)	Langmuir model			Freundlich model		
		q_m (mg g ⁻¹)	K_b (L mg ⁻¹)	R^2	K_F (mg g ⁻¹)	n	R^2
TC	30	133.33	2.5	0.9917	97.08	2.95	0.7925
	45	434.78	1.434	0.9880	256.16	8.40	0.1314
	60	435.00	1.52	0.9968	145.91	2.52	0.9316
OTC	30	101.01	0.172	0.9758	1.06	2.74	0.9303
	45	109.89	0.291	0.9724	1.03	2.41	0.6731
	60	149.25	0.163	0.9638	1.04	2.08	0.8503
CTC	30	100.00	0.77	0.9796	52.35	3.77	0.6660
	45	99.00	0.88	0.9773	25.24	2.98	0.7241
	60	101.01	1.39	0.9575	53.94	4.25	0.4240

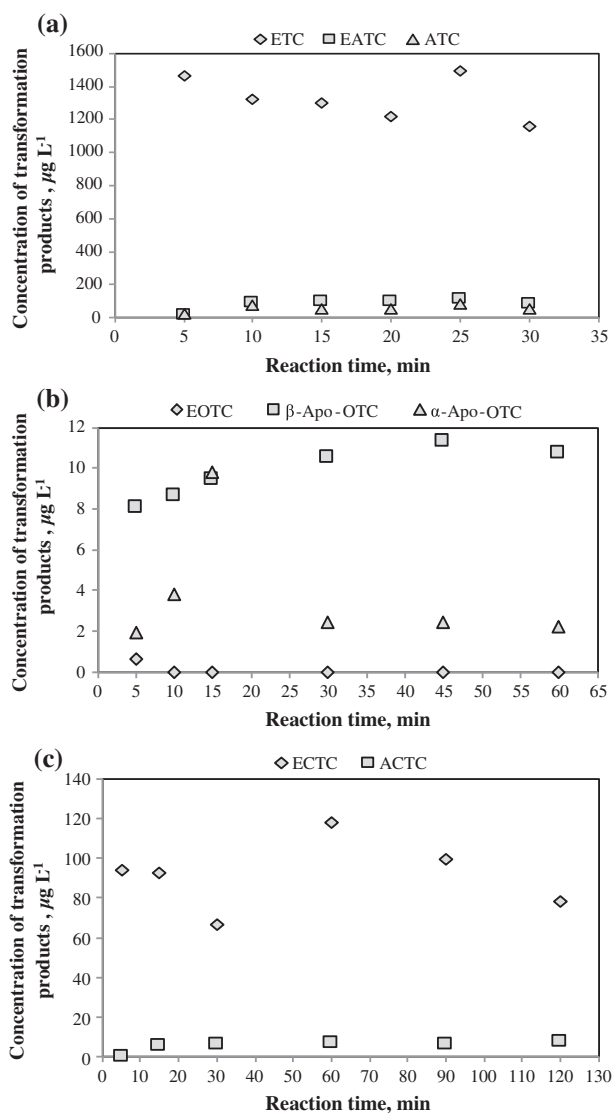


Fig. 9. The concentration of TC (a), OTC (b), and CTC (c) transformation products during the reaction time (conditions: pH 6, $C_{0(\text{TCs})} = 60 \text{ mg L}^{-1}$, ZVI dosage = 0.2 g L^{-1} (for TC), 0.6 g L^{-1} (for OTC and CTC)).

4. Conclusions

In this work, nanoscale Cu/Fe bimetallic particle was used for removal of tetracycline antibiotics from aqueous solution. Removal of TCs was higher at pH 6 comparing other pH values due to electrostatic interaction. The removal efficiency for three TCs was increased when the bimetallic particle dosage was increased. The maximum adsorption capacity was increased with an increase in temperature. The maximum adsorption capacities of TCs on bimetallic particle were 435, 149.25, and 101.01 for TC, OTC, and CTC, respectively. The pseudo-second-order model fits

the adsorption kinetics of TCs on nanoscale bimetallic Cu/Fe particle. The adsorption isotherm data for bimetallic Cu/Fe particle fitted Langmuir model. The concentrations of transformation products were low as negligible as and the dominant transformation products of TC, OTC, and CTC are ETC, β-Apo-OTC, ECTC, respectively. The desorbed amounts of TCs were above 50%. The results obtained from this study indicated that the removal mechanism of TCs was mainly due to adsorption on nanoscale Cu/Fe bimetallic particle surface rather than degradation process. Nanoscale Cu/Fe bimetallic particle is a promising alternative for the treatment of water contaminated with antibiotics such as TCs.

Acknowledgment

This study was supported by project no. 111Y092 of TUBİTAK.

References

- [1] J. Jiang, Z. Zhou, Occurrence and transform of emerging micropollutants in the environment, analytical challenges and treatment technologies: A global case study, in: Proceedings of 12th International Conference on Environmental Science and Technology, Rhodes, Greece, September 8–10, 2011.
- [2] M. Carballa, F. Omil, J.M. Lema, M. Llompart, C. García, I. Rodríguez, M. Gómez, T. Ternes, Behaviour of pharmaceuticals and personal care products in a sewage treatment plant of northwest Spain, *Water Sci. Technol.* 52(8) (2005) 29–35.
- [3] M. Carballa, F. Omil, J.M. Lema, Comparison of predicted and measured concentrations of selected pharmaceuticals, fragrances and hormones in Spanish sewage, *Chemosphere* 72 (2008) 1118–1123.
- [4] A. Wick, Occurrence and fate of emerging organic micropollutants in biological wastewater treatment, Dissertation, Zur Erlangung des akademischen Grades eines Doktors der Naturwissenschaften, Fachbereich 3: Mathematik/Naturwissenschaften, Universität Koblenz-Landau (2010).
- [5] J. Jeong, W. Song, W.J. Cooper, J. Jung, J. Greaves, Degradation of tetracycline antibiotics: Mechanisms and kinetic studies for advanced oxidation/reduction processes, *Chemosphere* 78 (2010) 533–540.
- [6] K. Kümmerer, Antibiotics in the aquatic environment – A review – Part I, *Chemosphere* 75 (2009) 417–434.
- [7] A.K. Sarmah, M.T. Meyer, A.B.A. Boxall, A global perspective on the use, sales, exposure pathways, occurrence, fate and effects of veterinary antibiotics (VAs) in the environment, *Chemosphere* 65 (2006) 725–759.
- [8] Y. Lin, S. Xu, J. Li, Fast and highly efficient tetracyclines removal from environmental waters by graphene oxide functionalized magnetic particles, *Chem. Eng. J.* 225 (2013) 679–685.
- [9] B. Halling-Sørensen, S.N. Nors Nielsen, P.F. Lanzky, F. Ingwerslev, H.C.H. Lützhøft, S.E. Jørgensen,

- Occurrence, fate and effects of pharmaceutical substances in the environment – A review, *Chemosphere* 36(2) (1998) 357–393.
- [10] Z.H. Li, L. Schulz, C. Ackley, N. Fenske, Adsorption of tetracycline on kaolinite with pH-dependent surface charges, *J. Colloid Interface Sci.* 351 (2010) 254–260.
- [11] H. Liu, Y. Yang, J. Kang, M. Fan, J. Qu, Removal of tetracycline from water by Fe-Mn binary oxide, *J. Environ. Sci.* 24(2) (2012) 242–247.
- [12] K. Li, A. Yediler, M. Yang, S. Schulte-Hostede, M.H. Wong, Ozonation of oxytetracycline and toxicological assessment of its oxidation by-products, *Chemosphere* 72 (2008) 473–478.
- [13] M.H. Khan, H. Bae, J.Y. Jung, Tetracycline degradation by ozonation in the aqueous phase: Proposed degradation intermediates and pathway, *J. Hazard. Mater.* 181(1–3) (2010) 659–665.
- [14] K.J. Choi, H.-J. Son, S.H. Kim, Ionic treatment for removal of sulfonamide and tetracycline classes of antibiotic, *Sci. Total Environ.* 387 (2007) 247–256.
- [15] K.J. Choi, S.G. Kim, S.H. Kim, Removal of antibiotics by coagulation and granular activated carbon filtration, *J. Hazard. Mater.* 151 (2008) 38–43.
- [16] J. Rivera-Utrilla, C.V. Gómez-Pacheco, M. Sánchez-Polo, J.J. López-Peñalver, R. Ocampo-Pérez, Tetracycline removal from water by adsorption/bioadsorption on activated carbons and sludge-derived adsorbents, *J. Environ. Manage.* 131 (2013) 16–24.
- [17] L. Zhang, X.Y. Song, X.Y. Liu, L.J. Yang, F. Pan, J. Lv, Studies on the removal of tetracycline by multi-walled carbon nanotubes, *Chem. Eng. J.* 178 (2011) 26–33.
- [18] R.W. Gillham, S.F. O'Hannesin, Enhanced degradation of halogenated aliphatics by zero-valent iron, *Ground Water* 32 (1994) 958–967.
- [19] X. Lv, Y. Hu, J. Tang, T. Sheng, G. Jiang, X. Xu, Effects of co-existing ions and natural organic matter on removal of chromium(VI) from aqueous solution by nanoscale zero valent iron (nZVI)-Fe₃O₄ nanocomposites, *Chem. Eng. J.* 218 (2013) 55–64.
- [20] C.B. Wang, W.X. Zhang, Synthesizing nanoscale iron particles for rapid and complete dechlorination of TCE and PCBs, *Environ. Sci. Technol.* 31(7) (1997) 2154–2156.
- [21] S. Luo, P. Qin, J. Shao, L. Peng, Q. Zeng, J. Gu, Synthesis of reactive nanoscale zero valent iron using rectorite supports and its application for orange II removal, *Chem. Eng. J.* 223 (2013) 1–7.
- [22] X. Ling, J. Li, W. Zhu, Y. Zhu, X. Sun, J. Shen, W. Han, L. Wang, Synthesis of nanoscale zero-valent iron/ordered mesoporous carbon for adsorption and synergistic reduction of nitrobenzene, *Chemosphere* 87 (2012) 655–660.
- [23] R.A. Crane, T.B. Scott, Nanoscale zero-valent iron: Future prospects for an emerging water treatment technology – Review, *J. Hazard. Mater.* 211–212 (2012) 112–125.
- [24] E. Keane, Fate, transport, and toxicity of nanoscale zero-valent iron (nZVI) used during superfund remediation, US Environmental Protection Agency Office of Solid Waste and Emergency Response Office of Superfund Remediation and Technology Innovation, Washington, DC, 2009.
- [25] A. Ghauch, A. Tuqan, H.A. Assi, Antibiotic removal from water: Elimination of amoxicillin and ampicillin by microscale and nanoscale iron particles, *Environ. Pollut.* 157 (2009) 1626–1635.
- [26] D. O'Carroll, B. Sleep, M. Krol, H. Boparai, C. Kocur, Nanoscale zero valent iron and bimetallic particles for contaminated site remediation, *Adv. Water Resour.* 51 (2013) 104–122.
- [27] X. Li, D.W. Elliott, W. Zhang, Zero-valent iron nanoparticles for abatement of environmental pollutants: Materials and engineering aspects, *Crit. Rev. Solid State Mater. Sci.* 31 (2006) 111–122.
- [28] G.A. Mansoori, T. Rohani Bastami, A. Ahmadpour, Z. Eshaghi, Environmental application of nanotechnology, Chapter 2, *Annu. Rev. Nano Res.* 2 (2008) 1–73.
- [29] K.D. Grieger, A. Fjordbøge, N.B. Hartmann, E. Eriksson, P.L. Bjerg, A. Baun, Environmental benefits and risks of zero-valent iron nanoparticles (nZVI) for *in situ* remediation: Risk mitigation or trade-off? *J. Contam. Hydrol.* 118 (2010) 165–183.
- [30] W.J. Liu, T.T. Qian, H. Jiang, Bimetallic Fe nanoparticles: Recent advances in synthesis and application in catalytic elimination of environmental pollutants, *Chem. Eng. J.* 236 (2014) 448–463.
- [31] Z.Q. Fang, X.H. Qiu, J.H. Chen, X.Q. Qiu, Degradation of metronidazole by nanoscale zero-valent metal prepared from steel pickling waste liquor, *Appl. Catal. B: Environ.* 100 (2010) 221–228.
- [32] Z.Q. Fang, J.H. Chen, X.H. Qiu, X.Q. Qiu, W. Cheng, L.C. Zhu, Effective removal of antibiotic metronidazole from water by nanoscale zero-valent iron particles, *Desalination* 268 (2011) 60–67.
- [33] G.G. Raja, R. Parthiban, K. Pandian, Effective removal of antibiotic metronidazole from water by using bimetallic nanoparticles, *J. Innov. Res. Sol. (JIRAS)* 1(1) (2014) 245–253.
- [34] C. Gu, K.G. Karthikeyan, S.D. Sibley, J.A. Pedersen, Complexation of the antibiotic tetracycline with humic acid, *Chemosphere* 66 (2007) 1494–1501.
- [35] Y.H. Hwang, D.G. Kim, H.S. Shin, Effects of synthesis conditions on the characteristics and reactivity of nanoscale zero valent iron, *Appl. Catal. B* 105 (2011) 144–150.
- [36] J.P. Fennelly, A.L. Roberts, Reaction of 1,1,1-trichloroethane with zero-valent metals and bimetallic reductants, *Env. Sci. Technol.* 32 (1998) 1980–1988.
- [37] K.V. Kumar, K. Porkodi, Mass transfer, kinetics and equilibrium studies for the biosorption of methylene blue using *Paspalum notatum*, *J. Hazard. Mater.* 146 (2007) 214–226.
- [38] Z. Qiang, C. Adams, Potentiometric determination of acid dissociation constants (pKa) for human and veterinary antibiotics, *Water Res.* 38(12) (2004) 2874–2890.
- [39] C. Gu, K.G. Karthikeyan, Interaction of tetracycline with aluminum and iron hydrous oxides, *Env. Sci. Technol.* 39 (2005) 2660–2667.
- [40] E. Tanis, K. Hanna, E. Emmanuel, Experimental and modeling studies of sorption of tetracycline onto iron oxides-coated quartz, *Colloids Surf. A* 327 (2008) 57–63.
- [41] H. Chen, H. Luo, Y. Lan, T. Dong, B. Hu, Y. Wang, Removal of tetracycline from aqueous solutions

- using polyvinylpyrrolidone (PVP-K30) modified nanoscale zero valent iron, *J. Hazard. Mater.* 192 (2011) 44–53.
- [42] Y.J. Shi, X.H. Wang, Z. Qi, M.H. Diao, M.M. Gao, S.F. Xing, S.G. Wang, X.C. Zhao, Sorption and biodegradation of tetracycline by nitrifying granules and the toxicity of tetracycline on granules, *J. Hazard. Mater.* 191 (2011) 103–109.
- [43] P.H. Chang, Z. Li, J.S. Jean, W.T. Jiang, C.J. Wang, K.H. Lin, Adsorption of tetracycline on 2:1 layered non-swelling clay mineral illite, *Appl. Clay Sci.* 67–68 (2012) 158–163.
- [44] N. Liu, M. Wang, M. Liu, F. Liu, L. Weng, L.K. Koopal, W. Tan, Sorption of tetracycline on organo-montmorillonites, *J. Hazard. Mater.* 225–226 (2012) 28–35.
- [45] Y. Gao, Y. Li, L. Zhang, H. Huang, J. Hu, S.M. Shah, X. Su, Adsorption and removal of tetracycline antibiotics from aqueous solution by graphene oxide, *J. Colloid Interf. Sci.* 368 (2012) 540–546.
- [46] Ö. Hanay, H. Türk, Comprehensive evaluation of adsorption and degradation of tetracycline and oxytetracycline by nanoscale zero-valent iron, *Desalin. Water Treat.* (2013) 1–9.
- [47] M.S. Chiou, H.Y. Li, Equilibrium and kinetic modeling of adsorption of reactive dye on cross linked chitosan beads, *Chemosphere* 50 (2002) 1095–1105.
- [48] A. Jia, Y. Xiao, J. Hu, M. Asami, S. Kunikane, Simultaneous determination of tetracyclines and their degradation products in environmental waters by liquid chromatography-electrospray tandem mass spectrometry, *J. Chromatogr. A* 1216 (2009) 4655–4662.